J Mater Sci: Mater Electron (2015) 26:2709–2712
DOI 10.1007/s10854-015-2746-4

Effects of Nb_2O_5 addition on the microstructure and dielectric properties of $BaTiO_3$–$Bi_{0.5}Na_{0.5}TiO_3$ ceramics

Yonggang Zhang · Shunqi Gao · Baolin Zhang

Received: 7 October 2014 / Accepted: 22 January 2015 / Published online: 1 February 2015

Abstract The influence of Nb_2O_5 on the microstructure and dielectric properties, including temperature dependence of permittivity, dielectric loss, and Curie temperature, has been investigated on $BaTiO_3$–$Bi_{0.5}Na_{0.5}TiO_3$ (abbreviated as BBT) ceramics. Experiments reveal that incorporation of a proper content of Nb_2O_5 in BBT ceramics can control the grain growth, reduce the dielectric loss, shift the Curie temperature to higher temperatures and significantly improve temperature characteristics of the $BaTiO_3$–$Bi_{0.5}Na_{0.5}TiO_3$ ceramics. As a result, a novel X10R material is developed in the system, which is very promising for practical use in X10R multilayer ceramic capacitors. With the addition of 2.0 wt% Nb_2O_5, the ceramics sintered at 1,150 °C showed favorable dielectric properties at 25 °C ($\varepsilon_r = 1{,}730$, $\tan\delta = 1.39 \times 10^{-2}$, and TCC = 12.0 %).

1 Introduction

Multilayer ceramic chip capacitors have been widely utilized as miniature-sized, high capacitance, and high reliability electronic components. In accordance with increasing demands for high-performance electronic equipment, multilayer ceramic chip capacitors also have encountered marketplace demand for small size, higher capacitance, lower cost, and high reliability [1–3]. A lot of attention has thus been given to the EIA-X10R specification, in which the temperature coefficient of capacitance (TCC) is within ±15 % of room temperature capacitance in the range of −55 to 250 °C.

The Pb(Ti, Sn)O_3 [4–6] system has been commonly used for X10R MLCCs. However, this composition should be replaced because Pb is very poisonous. Currently, the development of X10R MLCCs focuses on $BaTiO_3$-based ceramics. $BaTiO_3$ does not meet the thermal stability requirement (TCC = ±15 %) because the dielectric constant decreases dramatically when the Curie temperature is exceeded at 130 °C. $BaTiO_3$–$Bi_{0.5}Na_{0.5}TiO_3$ [7, 8] systems modified by Nb_2O_5 [8] (or MgO [9], Pr_6O_{11} [10]) have been investigated for preparation of X9R MLCCs with Pd or Pd/Ag as inner electrodes. Jing Wang et al. [11] used a two-step soft chemical method to synthesize $Ba_{0.985}Bi_{0.01}TiO3$–$BaTi_{0.98}Sn_{0.02}O_3$. They demonstrated that ceramics with core–shell [12, 13] structure could be easily obtained by using these uniformly distributed powders. In addition, the $BaTiO_3$–Nb_2O_5–Co_3O_4 [14, 15] and $BaTiO_3$–Nb_2O_5–Ni_2O_3 [16, 17] composition has been explored for X9R MLCCs.

In this work, we investigated Nb_2O_5 addition on the dielectric properties of $BaTiO_3$–$Bi_{0.5}Na_{0.5}TiO_3$ ceramics, in order to clarify the origin of the relatively flat and high dielectric constant temperature characteristics of $BaTiO_3$ based low firing temperature X10R capacitor materials.

2 Experiments

The samples used in this study were prepared by solid-state reaction. The original materials were reagent-grade

Y. Zhang (✉)
College of Mechanics, Taiyuan University of Technology, Taiyuan 030024, China
e-mail: yongzhizui2222@126.com

S. Gao
Institute of Electronics and Information Engineering, Tianjin University, Tianjin 300072, China

B. Zhang
Beijing Spacecrafts, Beijing 100094, China

$BaTiO_3$, Nb_2O_5, TiO_2, Bi_2O_3 and Na_2CO_3. The reagent-grade $BaTiO_3$ with Ba/Ti = 1.000 ± 0.005, calcined at 910 °C for 6 h. TiO_2, Bi_2O_3 and Na_2CO_3 powders were mixed according to $Bi_{0.5}Na_{0.5}TiO_3$ ceramics and milled with zirconia balls (Φ1 mm) for 6 h in distilled water. All the slurries were dried and calcined at 900 °C for 2 h. Two kinds of calcined powders with different amount of Nb_2O_5 additions were mixed according to the composition $xNbO_5$–$0.9BaTiO_3$–$0.1Bi_{0.5}Na_{0.5}TiO_3$ ceramics which is close to morphotropic phase boundary and re-milled for 8 h with ethanol as a dispersant. After drying, the powders were pressed into 10 mm diameter and 5 mm thickness pellets. Then these pellets were sintered at temperatures of 1,150 °C for 2 h.

The crystalline phases were identified by an X-ray diffractometer (Model 2038X, Rigaku Co.) with Cu Kα radiation. Microstructures of the sintered samples were observed with Scanning Electron Microscopy (SEM, Model Hitachi X-650). The ε_r and tanδ were measured by Agilent 4278 Capacitance Meter at 1 kHz, with temperature range of −55 to 250 °C. The TCC value is calculated by using the equation $\Delta C/C_{25\ ^\circ C} = (C - C_{25\ ^\circ C})/C_{25\ ^\circ C} \times 100\ \%$, where C and $C_{25\ ^\circ C}$ represented the capacitance value at measuring temperature and 25 °C respectively.

3 Results and discussion

The X-ray diffraction patterns of the BBT-x wt% Nb_2O_5 ceramics with $1 \leq x \leq 2.5$ sintered at 1,150 °C for 2 h were shown in Fig. 1. The main crystal phases of all the samples could be indexed by $BaTiO_3$ crystal structures. The crystal structure of $BaTiO_3$ is known as ABO_3 type perovskite [18, 19] structure with lattice parameter $a_0 = b_0 = 3.9823$ Å, $c_0 = 3.9891$ Å. However, a trace of two second phases, identified as $Ba_6Ti_{17}O_{40}$ and $Ba_6Ti_{14}Nb_2O_{39}$, are detected in the sample with 2.0–2.5 wt% Nb_2O_5. It has been assumed, therefore, that the solubility of Nb in BBT is below 2.5 wt%. As an B-site substitute, Nb^{5+} occupies the B-site and acts as an acceptor due to the size of the ionic diameter. This leads to the formation of cation vacancies to neutralize the electrical system. It is suggested by Hennings [20] that the Ti-site vacancies increase with higher Nb_2O_5 content, resulting in the instability of the BBT structure which precipitates second phase $Ba_6Ti_{14}Nb_2O_{39}$.

Figure 2 shows surface morphologies of the Nb_2O_5-doped BBT ceramics, revealing grain and grain boundary microstructure. All the samples show homogeneous fine-grained microstructures. The mean grain size of BBT ceramics gradually increased when doping with 1.0–2.0 wt% Nb_2O_5 for the sample. However, when the

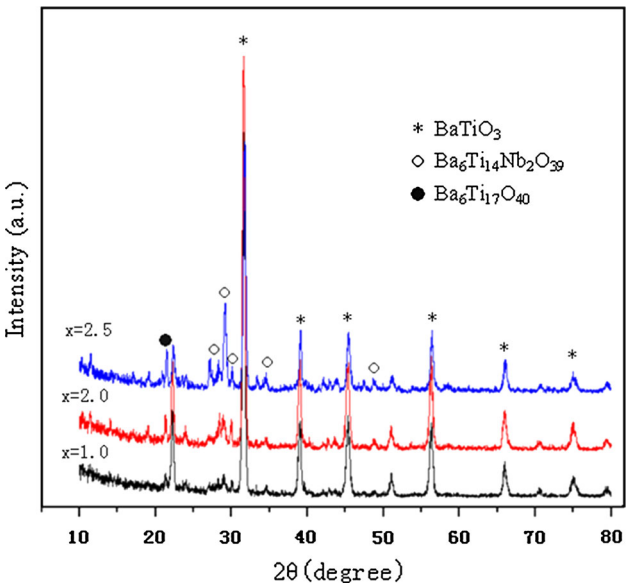

Fig. 1 XRD patterns of BBT ceramics with Nb_2O_5 addition sintered at 1,150 °C as a function of the Nb_2O_5 content

Nb_2O_5 content increases further to 2.0 wt%, a significant reduction in grain size is observed, which may result from the presence of a grain growth inhibiting second phase such as $Ba_6Ti_{14}Nb_2O_{39}$, as shown in Fig. 1. The particle's morphology is nearly cubic and the grain size is about 1 μm as seen in Fig. 2d.

The relative dielectric constant and dielectric loss of BBT ceramics sintered at 1,150 °C for 2 h are plotted in Fig. 3 as a function of added Nb_2O_5 content. As the amount of Nb_2O_5 increases, the ε_r value of the specimens decreases gradually, which is attributed to the low ε_r value of $Ba_6Ti_{17}O_{40}$ and $Ba_6Ti_{14}Nb_2O_{39}$. The tanδ decreased with increasing Nb_2O_5 content, together with the XRD and SEM results, suggesting that the variation of tanδ was mainly related to its phase composition and microstructure. Meanwhile, the minimum dielectric loss was obtained as the addition of Nb_2O_5 content were 2.5 wt%.

Figure 4 shows the temperature dependence of dielectric constant for samples with various amounts of Nb_2O_5. The curve of the sample without Nb_2O_5 presents an obvious dielectric constant peak at about 130 °C, just as pure $BaTiO_3$. For the sample with 1.0–2.5 wt% Nb_2O_5, the peak is shifted to 150 °C. The transition point of Nb-doped BBT is about 150 °C, much lower than that of pure BBT, which is about 165 °C. Figure 1 shows a set of XRD patterns of samples doped with various amount of Nb_2O_5. The main phase is referred to $BaTiO_3$. The secondary phases are identified as Ti–rich phases, such as $Ba_6Ti_{17}O_{40}$ and $Ba_6Ti_{14}Nb_2O_{39}$. It indicates that Nb^{5+} mainly enters the Ti-sites as a donor. According to Datta et al. [21], the high-transition temperature of BBT solid solutions can be

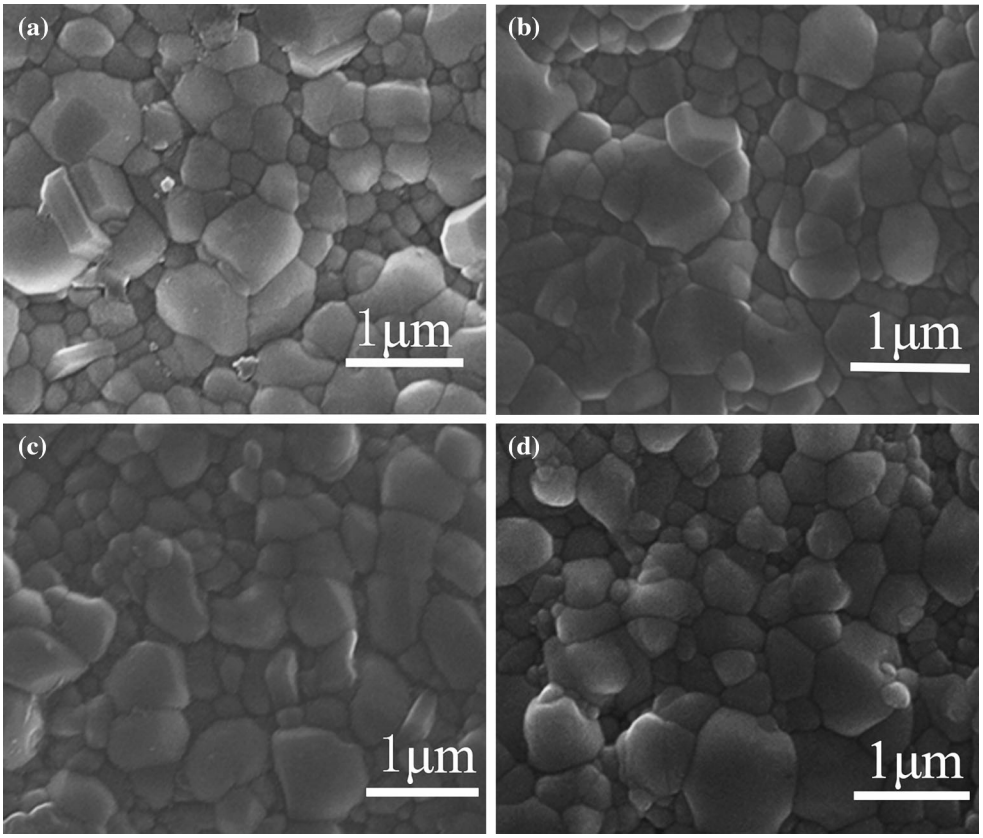

Fig. 2 Micrographs of BBT ceramics with Nb_2O_5 addition at **a** 1.0 wt%, **b** 1.5 wt%, **c** 2.0 wt% and **d** 2.5 wt% at 1,150 °C

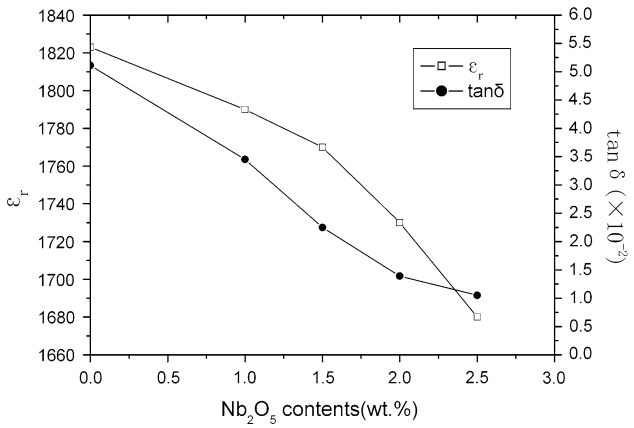

Fig. 3 Dielectric constants and tanδ values of BBT-x wt% Nb_2O_5 ceramics sintered at 1,150 °C

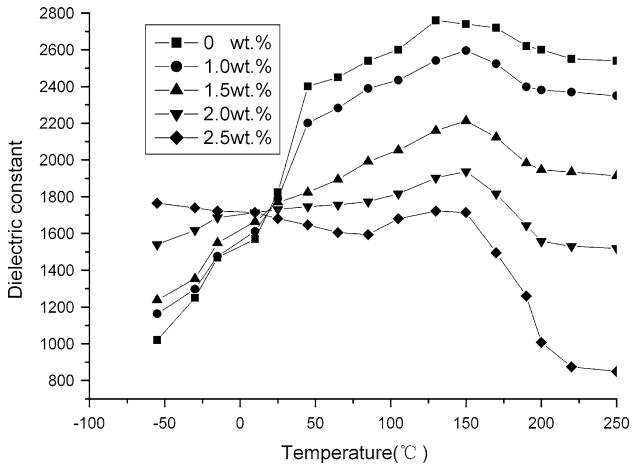

Fig. 4 Temperature dependence of dielectric constant for samples with various amounts of Nb_2O_5

attributed to the shortening of the Ti–O bonds. Therefore, the decrease of Tc in Nb-doped BTBNT should be ascribed to the generation of Ti vacancies [21, 22]. With the continued increasing Nb_2O_5 content, the curve shape changes greatly, and meanwhile, the dielectric constant is markedly enhanced at lower temperature. In the case of 2.0 and 2.5 wt% Nb_2O_5, the peak at about 150 °C is supressed. The change is beneficial to the improvement of temperature stability, especially in the high-temperature range (150–250 °C).

Figure 5 shows the effect of Nb_2O_5 contents on the TCC of BBT ceramics sintered at 1,150 °C. It was well known that the TCC value was governed by the composition, the additive, and the second phase of the materials [23–25]. As the added amount of Nb_2O_5 increased, The TCC shifted to

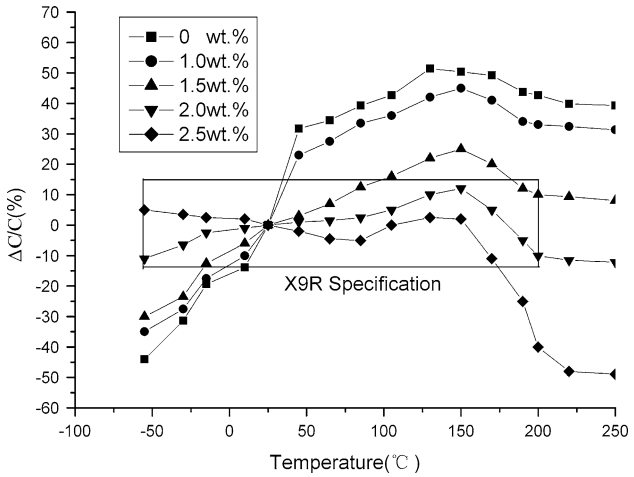

Fig. 5 Temperature coefficient of capacitance (TCC) of BBT ceramics with various amounts of Nb_2O_5

positive region in the range of −55 to 25 °C. While, The TCC shifted to negative region in the range of 25–250 °C. This is mainly attributed to the increase of $Ba_6Ti_{17}O_{40}$ and $Ba_6Ti_{14}Nb_2O_{39}$ phases due to the addition of Nb_2O_5. For the sample with 1.0 and 2.5 wt% Nb_2O_5, the capacitance variation rate is relatively large in the high-temperature range (150–250 °C). The maximum capacitance variation rate of the sample with 1.0 wt% Nb_2O_5 is even up to 45 %. When Nb_2O_5 doping content reaches to 2.0 wt%, the temperature stability is improved dramatically, especially in the high-temperature range. The maximum capacitance variation rate is down to only about 12 %, which can satisfy the broad temperature stability specification well. Obviously, the appropriate addition of Nb_2O_5 could be considered as a third phase which may affect the temperature dependence of the capacitance. With 2 wt% of Nb_2O_5, the TCC of BBT varied from −11.0 to 12.0 % in the range of −55 to 250 °C. Moreover, the permittivity of the sample without Nb_2O_5 increased with the temperature increasing (25–150 °C). Therefore the TCC can be dramatically reduced (from 25 to 150 °C) with 2.5 % doping of niobium oxide though the permittivity only reduces by 10 %.

4 Conclusions

The dielectric properties and microstructure of BBT ceramics with different amounts of Nb_2O_5 additives were investigated to develop a new X10R for use in multilayer ceramic capacitors. The BBT ceramics with 1.0–2.5 wt% Nb_2O_5 additives were well-sintered at around 1,150 °C. For the samples doped with 2.0 wt% Nb_2O_5, good dielectric properties of $\varepsilon_r = 1{,}730$, $\tan\delta = 1.39 \times 10^{-2}$, and TCC = 12.0 % were obtained when sintered at 1,150 °C for 2 h.

References

1. J. Koch, K. Seidel, W. Weinreich, Microelectron. Eng. **109**, 148 (2013)
2. X.J. Wu, Y.J. Wang, Q.X. Zeng, Proc. Eng. **45**, 998 (2012)
3. J. Virkki, A. Koskenkorva, L. Frisk, Microelectron. Reliab. **50**, 1711 (2013)
4. S.Q. Gao, S.H. Wu, Y.G. Zhang, Mater. Sci. Eng. B **176**, 68 (2011)
5. C. He, X.Z. Li, Z.J. Wang, Ceram. Int. **39**, 853 (2013)
6. S.F. Wang, J.H. Li, Y.F. Hsu, J. Eur. Ceram. Soc. **33**, 1793 (2013)
7. Y. Sun, H. Liu, H. Hao, Ceram. Int. **38**, S41 (2012)
8. G. Yao, X. Wang, Y. Zhang, J. Am. Ceram. Soc. **95**, 3525 (2012)
9. L.X. Li, M.J. Wang, Y.R. Liu, Ceram. Int. **40**, 1105 (2014)
10. C.L. Freeman, J.A. Dawson, H. Chen, J. Mater. Chem. **21**, 4861 (2011)
11. J. Wang, S.L. Jiang, D. Jiang, Ceram. Int. **38**, 5853 (2012)
12. M. Cernea, B.S. Vasile, A. Boni, J. Alloys Compd. **587**, 553 (2014)
13. C.H. Kim, K.J. Park, Y.J. Yoon, J. Eur. Ceram. Soc. **28**, 2589 (2008)
14. W. Li, J.Q. Qi, Y.L. Wang, Mater. Lett. **57**, 1 (2002)
15. B. Xiong, H. Hao, S.J. Zhang, Ceram. Int. **38**, S45 (2012)
16. A.W. Sleight, Prog. Solid State Chem. **37**, 251 (2009)
17. X.Q. Chen, J. Xiao, Y. Xue, Ceram. Int. **40**, 2635 (2014)
18. C.L. Tian, Z.X. Yue, Y.Y. Zhou, J. Solid State Chem. **197**, 242 (2013)
19. I. Popescu, A. Urda, T. Yuzhakova, C. R. Chim. **12**, 1072 (2009)
20. D. Hennings, G. Rosenstein, J. Am. Ceram. Soc. **67**, 249 (1984)
21. K. Datta, K. Roleder, P.A. Thomas, J. Appl. Phys. **106**, 123512 (2009)
22. G.F. Yao, X.H. Wang, Y.Y. Wu, J. Am. Ceram. Soc. **95**, 614 (2012)
23. B.W. Lee, I.R. Abothu, P.M. Raj, Scripta Mater. **54**, 1231 (2006)
24. S.U. Park, C.Y. Kang, H.M. Kwon, Microelectron. Eng. **88**, 3389 (2011)
25. S. Vangchangyia, T. Yamwong, E. Swatsitang, Ceram. Int. **39**, 8133 (2013)